Synchronization in complex networks with a modular structure

Kwangho Park, Ying-Cheng Lai,[a] and Saurabh Gupte
Department of Electrical Engineering, Arizona State University, Tempe, Arizona 85287

Jong-Won Kim
Department of Mathematics, Arizona State University, Tempe, Arizona 85287

(Received 30 August 2005; accepted 28 November 2005; published online 31 March 2006)

Networks with a community (or modular) structure arise in social and biological sciences. In such a network individuals tend to form local communities, each having dense internal connections. The linkage among the communities is, however, much more sparse. The dynamics on modular networks, for instance synchronization, may be of great social or biological interest. (Here by synchronization we mean some synchronous behavior among the nodes in the network, not, for example, partially synchronous behavior in the network or the synchronizability of the network with some external dynamics.) By using a recent theoretical framework, the master-stability approach originally introduced by Pecora and Carroll in the context of synchronization in coupled nonlinear oscillators, we address synchronization in complex modular networks. We use a prototype model and develop scaling relations for the network synchronizability with respect to variations of some key network structural parameters. Our results indicate that *random, long-range links among distant modules* is the key to synchronization. As an application we suggest a viable strategy to achieve synchronous behavior in social networks. © *2006 American Institute of Physics*.
[DOI: 10.1063/1.2154881]

We are familiar with the following situation in daily life: when two people are introduced, they often discover quickly that they have social connections, e.g., they share common friends, etc. Considering the typically large size of the communities and the limited number of acquaintances a person has, this happens with a surprisingly high probability, even if people systematically underestimate the likelihood of coincidences. The often successful identification of acquaintances is even more striking in view of the very small number of friends usually mentioned in the introductory conversation. This problem is related to the small-world phenomenon,[1] according to which any two people are connected by a short chain of acquaintances. The existence of short paths in these systems has been successfully described by network models with some degree of randomness. Short paths are present, however, in most random networks. Social networks thus must necessarily possess unique structures that are *not* present in random networks. The pioneering work of Watts, Dodds, and Newman[2] identified *modular structure* as an essential ingredient for social networks. In particular, individuals in a society tend to form groups according to their social characteristics. Within a group, connections are dense in the sense that each member is connected to almost all other members in the group, while connections among different groups are typically sparse. Although originated in social sciences, recent works have indicated that modular networks are important for biological networks such as metabolic networks[3] and protein interaction graphs.[4,5] Synchronized behavior in a modular network may be of great interest. For instance, the outcome of a general election may be easily altered due to some naturally or organized synchronous behavior in some social networks. This represents an interdisciplinary problem to which knowledge and tools from nonlinear physics, particularly those developed from network science and nonlinear dynamics, can be applied. This paper presents a systematic study of synchronization in modular networks. By utilizing a general theoretical framework for addressing synchronization in complex networks and a class of prototype models for modular networks, we have obtained quantitative scaling results relating the network synchronizability to some key parameters characterizing the network structure. The results suggest that, for a modular network to achieve synchronization, it is advantageous to establish and enhance random connections amongst distant communities rather than those amongst nearby or within individual communities.

I. INTRODUCTION

In their seminal work, Watts and Strogatz[1] showed that the addition of a small number of shortcut links to a regular, locally connected network can greatly reduce the average network distance between two nodes while keeping the network locally clustered. Such networks are said to have the small-world (SW) property. Many examples from real-world networks including both artificial and natural systems have been identified to have the SW property. Another seemingly generic feature of networks in the real world is the scale-free (SF) nature of the connectivity distribution, as signified by a power-law form. Barabási and Albert[6] suggested a model of growing networks (BA model), in which preferential attachment of new links to nodes with higher connectivity results

[a]Electronic mail: yclai@chaos1.la.asu.edu

in the SF property. SF networks have particularly small average network distance due to the heterogeneity in the connectivity distribution.

The structural properties of a complex network can affect the dynamical processes taking place on it, such as synchronization. There have been recent efforts in this direction.[7–11] For instance, it was found[9] that networks with a homogeneous distribution of connectivity are more synchronizable than heterogeneous ones (e.g., scale-free networks), even though the average network distances of the former are larger. Some degree of homogeneity is then expected in naturally evolved structures, such as neural networks, where synchronizability is desirable. It was also found[10,11] that synchronizability is generally improved in weighted networks, networks in which the strengths of links are not uniform.

The structure of social networks is characteristically different from those of regular, small-world, scale-free, and random networks.[2,12] In a social network, people are clustered into groups on the basis of social characteristics or interests. Usually, the density of links (the average number of links per node) within each group is much higher than that among distinct groups. This type of modular structure can explain familiar social experiences such as the quick identification of acquaintances, as follows. Once two people are introduced, they describe themselves in terms of their social characteristics (e.g., profession, place of work, and leisure activities, etc.). Next, each of them cites friends with social characteristics "close" to those of the other person. This is, actually, a second step in the process of introduction, but can be effectively seen as an attempt to find chains of acquaintances linking them. The success of this attempt depends on the modular structure of the social network. The modular or community structure has also been identified in biological sciences and is important, e.g., for metabolic networks[3] and protein interaction graphs.[4,5]

In this paper, we address synchronization in complex modular networks. (Here by synchronization we mean some synchronous behavior among the nodes in the network, not, for example, partially synchronous behavior in the network or the synchronizability of the network with some external dynamics.) Synchronized behavior of a number of individuals can have significant social or political impacts. For instance, the outcome of a general election may be the result of the synchronization in a social network with modular structure. Thus understanding how a modular network attains synchronization is a subject of broad interest.[13] Our approach is to construct a class of idealized, quasi-one-dimensional modular networks that are amenable to analysis. Using linear stability analysis[14] and its generalization,[7,15] we are able to obtain theoretical scaling results and verify them for more general networks. In particular, note that, for a modular network, the key parameters are the number of modules and the probability for links among different modules (e.g., long-range links). Our results concern how the network synchronizability depends on these parameters. We find that connectivities within individual modules have little impact on the synchronizability. It is easier to synchronize the network with increasing number of modules when there are *random*, long-range links among the modules. However, this trend is reversed when the modules are connected locally: in this case it is more difficult to synchronize the network as the number of modules is increased. This suggests a phase-transition-like phenomenon. An implication for social networks is that to achieve synchronization it is advantageous to establish and enhance random connections amongst distant communities rather than those amongst nearby or individual communities.

In Sec. II, we review the basic framework of linear stability analysis as applied to synchronization in complex networks. In Sec. III, we present an idealized but analyzable model of modular network and derive scaling laws governing the dependence of the synchronizability on the key network parameters. In Sec. IV, we present results with three classes of more general modular networks, which provide support for our theory. Discussions are presented in Sec. V.

II. LINEAR STABILITY ANALYSIS

A powerful theoretical tool to analyze the synchronizability of large, complex networks is oscillator networks and linear stability analysis. Given a complex network of N nodes, one can imagine N oscillators, one placed at each node, coupled according to the network topology. The oscillators need to be identical to facilitate the stability analysis. Mathematically, a complex oscillator network can be described conveniently by a coupled differential-equation system, as follows:

$$\dot{\mathbf{x}}_i = \mathbf{F}(\mathbf{x}_i) + K\sum_{j=1}^{N} L_{ij}\mathbf{H}(\mathbf{x}_j), \quad i = 1, \cdots, N, \tag{1}$$

where $\mathbf{F}(\mathbf{x}_i)$ describes the d-dimensional, uncoupled dynamics of node i, K is coupling strength, L_{ij} is the coupling matrix determined by the connecting topology of the network, and $\mathbf{H}$ is a coupling function. The coupling matrix can be conveniently defined to be Laplacian: $L_{ij}=-1$ if node i and node j are connected, $L_{ii}=k_i$, if node i has k_i connections, and $L_{ij}=0$ otherwise. The matrix thus satisfies the conditions

$$\sum_{i=1}^{N} L_{ij} = 0, \quad \sum_{j=1}^{N} L_{ij} = 0. \tag{2}$$

This way, the Laplacian matrix can be written as $L=BB^T$ for some matrix B, and so all its eigenvalues are real and nonnegative. Since the rows of L have zero sum, the smallest eigenvalue is $\lambda_1=0$. As all nodes in the network are connected, we can conveniently arrange the eigenvalue spectrum of the matrix as

$$\lambda_1 = 0 < \lambda_2 \leqslant \ \ldots \ \leqslant \lambda_N.$$

Because all oscillators are assumed to be identical, the synchronization state (or the synchronization manifold) $\mathbf{x}_i(t) = \mathbf{s}(t)$ $(i=1, \ldots, N)$ is a solution of Eq. (1), which satisfies

$$\dot{\mathbf{s}} = \mathbf{F}(\mathbf{s}).$$

The linear stability of the synchronized state is determined by the corresponding variational equations, which can be diagonalized into N blocks, each of the form

$$\dot{\mathbf{y}}_i = [\mathbf{DF}(\mathbf{s}) + \lambda_i K \mathbf{DH}(\mathbf{s})]\mathbf{y}_i, \quad i = 1,2,\ldots,N, \tag{3}$$

where $\mathbf{y}$ represents different modes of perturbation from the synchronized state, or the perturbations in the subspaces transverse to the synchronization manifold. Note that Eq. (3) is a set of linear equations governing the evolution of the set of infinitesimal vectors $\mathbf{y}_i$ in the tangent space of the oscillator dynamics, which determines the subset of Lyapunov exponents for the dynamics in each block. Since $\lambda_1 = 0$, the first block is independent of the network coupling and, hence, it represents the dynamics in the d-dimensional synchronization manifold and the corresponding Lyapunov exponents are those associated with each individual oscillator. The remaining $N-1$ blocks govern the dynamics in the $(N-1)d$-dimensional transverse subspace, which determine the spectrum of $(N-1)d$ *transverse Lyapunov exponents*. Physically, synchronization occurs only when all the transverse exponents are negative. The largest transverse Lyapunov exponent, denoted by $\Lambda(\sigma)$, is called the *master stability function*,[15,16] where $\sigma \equiv \lambda_i K$ for $i = 2,\ldots,N$ denotes a generalized coupling-strength parameter.

The master stability function possesses one interesting property that is key to the synchronizability of a complex network of oscillators. Without loss of generality, we consider a network of coupled chaotic oscillators. For weak coupling that does not result in synchronization, the master stability function is positive. One can imagine that as the generalized coupling parameter is increased through a critical value, say σ_1, the master stability function becomes negative so that synchronization occurs. As the coupling is increased further, the function would become more negative, implying more stable synchronization. But can this trend continue indefinitely?

To address this question, we notice the roles of the coupling terms: (1) they serve to establish the coherence among oscillators, and (2) they are effectively perturbations to the dynamics of individual oscillators. Whether synchronization can occur depends on the interplay between these two factors. In particular, for small coupling, synchronization may not occur because, although the perturbing effect of the coupling terms is small, the amount of coherence provided by them is also small. For very large coupling, although the coupling terms can provide strong coherence, the effective perturbations are also large. As a large perturbation requires a longer time for the system to reach an equilibrium state (e.g., synchronization), in this case, the system will have no time to respond to the perturbations and consequently is unable to synchronize. Thus, synchronization may not occur if the coupling is too strong. In general, for a coupled oscillator system there exists a finite interval of the coupling parameter for which synchronization can occur.[15] In terms of the master stability function, these arguments suggest the existence of another critical value of the coupling parameter, say $\sigma_2 > \sigma_1$, above which the function becomes positive so that synchronization is lost. These considerations are reflected in Fig. 1, a schematic illustration of the master stability function versus the generalized coupling parameter σ. We see that synchronization can occur only when the coupling parameter σ falls in the interval (σ_1, σ_2). Indeed, this behavior

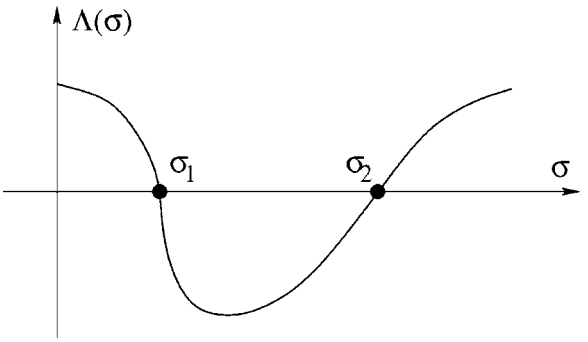

FIG. 1. Schematic illustration of the behavior of the master stability function vs the generalized coupling parameter σ for coupled oscillatory networks.

appears to be typical for a large class of coupled chaotic oscillatory systems.[15,16]

The synchronizability of a complex network of oscillators for any linear coupling scheme can be inferred from Fig. 1. A given network can be characterized by the set of eigenvalues (λ_2 through λ_N) of the corresponding Laplacian matrix, to which the generalized coupling parameter σ is proportional. For a fixed value of K, the spread of the eigenvalues determines the range of the possible variation in σ. This suggests a general quantity that determines the synchronizability of a complex network regardless of the detailed oscillator models: the *spread of the eigenvalues of the Laplacian matrix*. Referring to Fig. 1, we see that in order to achieve synchronization, the spread of the eigenvalues must not be too large to fit the generalized coupling parameter σ in the interval (σ_1, σ_2). That is, the synchronized state is linearly stable, if and only if

$$\lambda_N/\lambda_2 < \sigma_2/\sigma_1 \equiv \beta. \tag{4}$$

An interesting observation is that β is a constant that depends solely on $\mathbf{F}(\mathbf{x})$ that governs the node dynamics and the output function $\mathbf{H}(\mathbf{x})$. For various chaotic oscillators, the value of β ranges from 5 to 100.[7] The left-hand side of the inequality (4), the ratio λ_N/λ_2, depends only on the topology of interactions among oscillators. Hence, the impact of having a particular coupling topology on the network's ability to synchronize is represented by a single quantity λ_N/λ_2: the larger the ratio, the more difficult it is to synchronize the oscillators.

III. ANALYZABLE MODEL

To address the synchronizability of a modular network, it suffices to explore the relation between the eigenratio λ_N/λ_2 and the number of modules. To construct an analyzable model of a modular network, we imagine a network of N nodes grouped into M modules locating on a ring, each being connected to their nearest-neighbor modules, as shown in Fig. 2. The Laplacian matrix of the network is similar to that of a regular, "ring" network of N nodes. The eigenvector corresponding to the first nonzero eigenvalue of the ring network is

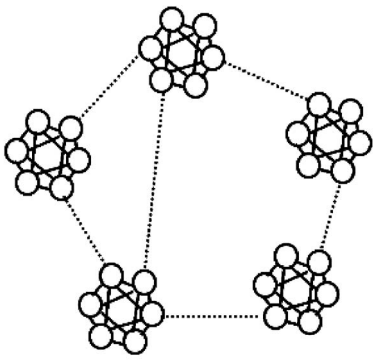

FIG. 2. Schematic illustration of a class of analyzable modular network. Within a module, nodes (circles) are densely connected to each other, modules are only sparsely connected (dotted lines).

$$\sqrt{2/N}[\sin(2\pi j/N)]_{j=1}^{N},$$

which can be considered as an envelope function of the eigenvectors in the modular network, as shown in Fig. 3. Since the variance of the components in a module is small compared to the difference between the means of two consecutive modules, we further approximate components within a module to have the same value and, as a result, the eigenvector of the network with M modules is given as a piecewise continuous step function,

$$\mathbf{v}_{2,M}^{t} = (\overbrace{h_M^1,\cdots,}^{N/M},\cdots,\overbrace{h_M^i,\cdots,h_M^i,}^{N/M}\cdots,\overbrace{\cdots,h_M^M}^{N/M}), \tag{5}$$

where all N/M components of the ith module have the same value $h_M^i = \sqrt{2/N}\sin(2\pi i/M)$. The first nonzero eigenvalue of the modular network is

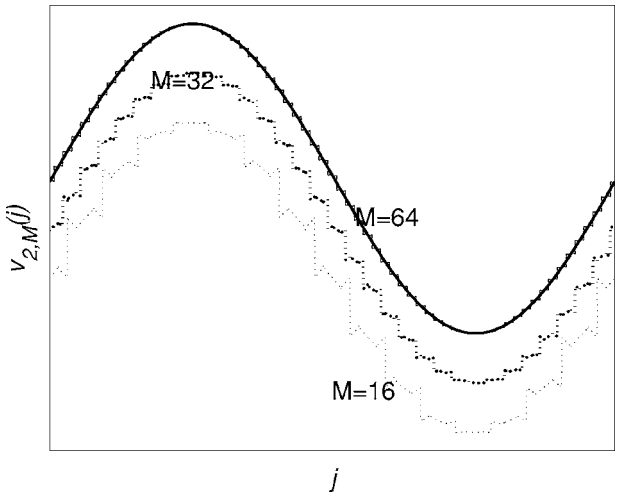

FIG. 3. Numerically obtained eigenvectors of the first nonzero eigenvalue $v_{2,M}$ for modular networks with different number of modules (in arbitrary units). Eigenvectors can be encapsulated by a single curve (thick solid line), $\sqrt{2/N}[\sin(2\pi j/N)]_{j=1}^{N}$, except for some small phase differences. Note that eigenvectors are shifted vertically.

$$\lambda_2 = \mathbf{v}_{2,M}^{t}\mathbf{L}\mathbf{v}_{2,M}, \tag{6}$$

where $\mathbf{L}$ is the Laplacian matrix of the network. Inserting Eq. (5) into Eq. (6), and assuming there are only two nearest connections per module, we obtain

$$\lambda_2 = \frac{2}{N}\sum_{i=1}^{M}\sin\left(\frac{i}{\theta_0}\right)\times\left[2\sin\left(\frac{i}{\theta_0}\right)-\sin\left(\frac{i-1}{\theta_0}\right)-\sin\left(\frac{i+1}{\theta_0}\right)\right], \tag{7}$$

where $\theta_0 = M/2\pi$. For $M \gg 1$, we have

$$\lambda_2 \approx \frac{4\pi}{NM}\int_0^{2\pi}\sin\theta(-\nabla^2\sin\theta)d\theta = \frac{4\pi^2}{NM}. \tag{8}$$

Although in general we cannot obtain an approximation for the largest eigenvalue in a similar way, we have known approximations for it in some special cases. For example, when the module is a regular "ring" network with $2k$ nearest connections, the largest eigenvalue of the module is $\lambda_{\max} \approx (2k+1)(1+2/3\pi)$.[17] Since $\lambda_{\max}$ depends on the number of nearest neighbors only, we may use the same $\lambda_{\max}$ as the largest eigenvalue of the network. (Although there is a small amount of increase in $\lambda_{\max}$ due to the connections between modules, we have numerically verified that the amount is less than 3% when M becomes $2M$.) Therefore, we obtain the ratio

$$\lambda_{\max}/\lambda_2 \approx (2k+1)(1+2/3\pi)NM/4\pi^2, \tag{9}$$

which indicates that the eigenratio increases linearly with M, as shown in Fig. 4(a). That is, with only local connections between modules, it is more difficult to achieve synchronization as the number of modules increases.

We can now consider a more general modular network model that allows long range interactions. That is, two arbitrary modules can make a connection with a probability $p(l)$, where l is the distance between modules. It is reasonable to assume that $p(l)$ has an exponential dependence on l,

$$p(l) = \exp(-\alpha l)/N_l, \tag{10}$$

where α is a parameter and N_l is a proper normalization constant. Inserting this $p(l)$ into Eq. (6) and again replacing the sum with an integral, we obtain

$$\lambda_2 \approx \frac{4\pi^2 K_0}{NM}\frac{\int_1^{M/2} l^2 e^{-\alpha l}dl}{\int_1^{M/2} e^{-\alpha l}dl}, \tag{11}$$

where the factor K_0 comes from the fact that each module can have multiple $(2K_0)$ connections. As an example, for the case of a "globally" connected modular network, we have $\alpha \to 0$ and $K_0 \sim M/2$. The integral ratio can then be simplified as M^2 and $\lambda_2 \sim M^2$. Thus, the eigenratio decreases as M increases:

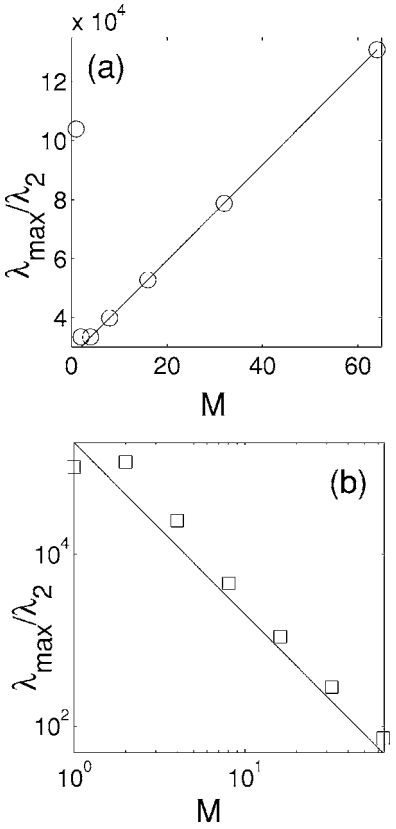

FIG. 4. Eigenratio vs the number of modules: (a) "ring" network where only two nearest neighbor modules are connected and (b) "globally" connected network where each module is connected to all the other modules. Circles and squares are numerically obtained eigenratios, while solid lines are from analytic solutions. The parameters are $N=4086$ and the number of nearest-neighbor connections is $2k=10$.

$$\lambda_{\max}/\lambda_2 \sim M^{-2}, \tag{12}$$

as shown in Fig. 4(b). This is opposite to the result in Fig. 4(a) where no long-range links among modules are allowed. Note that for $\alpha \to \infty$ and $K_0=1$, Eq. (11) becomes Eq. (8).

An interesting consequence of Eq. (11) is that a transition phenomenon occurs in the synchronizability of modular networks. For $\alpha \gtrsim 0$, connections between modules are *decentralized* and the integral ratio in Eq. (11) is proportional to M^2. As a result, the eigenratio decreases as M increases. However, for $\alpha \gg 0$, connections between modules are *centralized* among nearest neighbor modules and the integral ratio becomes independent of M for sufficiently large $M \gg \alpha^{-1}$ and the eigenratio eventually increases as M increases. We also expect a similar transition phenomenon when regarding K_0 as a function of M (i.e., $K_0 \sim M^{\eta}$). For example, suppose that $\alpha \to 0$ and the total number of connections between modules is fixed. Then K_0 is inversely proportional to M and, as a result, the eigenratio remains constant. Distinct synchronization behaviors can arise depending on the value of η.

Our considerations so far have been limited to the case where the parameter α is positive. From Eq. (10), we see that a relatively large, positive value of α stipulates smaller probabilities for long-range links among the modules as compared with those for short-range links. Thus, as α is increased from zero, long-range links become increasingly improbable, reducing the network synchronizability. An interesting question is what happens if α is negative. Intuitively, we expect that for a negative value of α, long-range links among modules can be much more probable than short-range links and, as a result, the network synchronizability should improve as α is decreased from zero. But is this really the case?

To gain insight, we use our ring modular-network model and generate different networks for visualization for several different values of α, as shown in Figs. 5(a)–5(c). For Fig. 5(a), the value of α is positive so that short-range links among the modules are favored. In this case, the average network distance can be large. For $\alpha=0$ [Fig. 5(b)], short-range and long-range links are equally probable, making the connections among modules small-world like with small average network distance. For $\alpha<0$, long-range links are favored, but the most favorable links are those squarely across the ring configuration. For example, for a circular ring, the modular links that are close to the diameter of the circle are the most favorable one, as shown in Fig. 5(c). This, in fact, makes the average network distance large. For networks with a similar topology, e.g., homogeneous networks with the small-world characteristics, the average network distance is the determining factor for synchronizability.[8,18] Thus, quite counterintuitively, as α becomes negative from a positive value, we expect the network synchronizability to increase and reaches maximum for $\alpha=0$, and then to decrease as α is decreased from zero.

For the ring modular-network configuration, estimates of the average network distance can be obtained for some limiting cases. In particular, for $\alpha \to \infty$, there is a strong tendency for a module to connect to only its nearest neighboring modules. For such a configuration with a large number (M) of modules, the average network distance is $d \sim M/4$. For $\alpha=0$, the probabilities for a module to connect to any other modules are equal, so the modular links appear random. In this case, the average network distance is $d \sim \ln M$, as for random networks.[19] In the limiting case where $\alpha \to -\infty$, there is a tendency that diametrically opposite modules are connected, as seen in Fig. 5(c), making most links nearly pass through the center of the ring configuration. In this case, the average network distance is $d \sim M/8$. For reasonably large values of M, we have

$$\ln M < M/8 < M/4,$$

suggesting that ring modular networks with α near zero are most synchronizable.

To provide numerical support, we examine how the synchronizability (as characterized by the eigenratio) and the average network distance vary with α, as shown in Fig. 6. The network consists of M modules, each containing five nodes that are connected in a one-to-all manner. For comparison, the link ratio (the ratio between the number of links among the modules and the total number of links in the network) is fixed at a small value (0.01 for Fig. 6). In Fig. 6(a), the eigenratio versus α is shown for three values of M. We see that for relatively large values of M, the eigenratio exhibits the expected behavior in that it decreases as α is

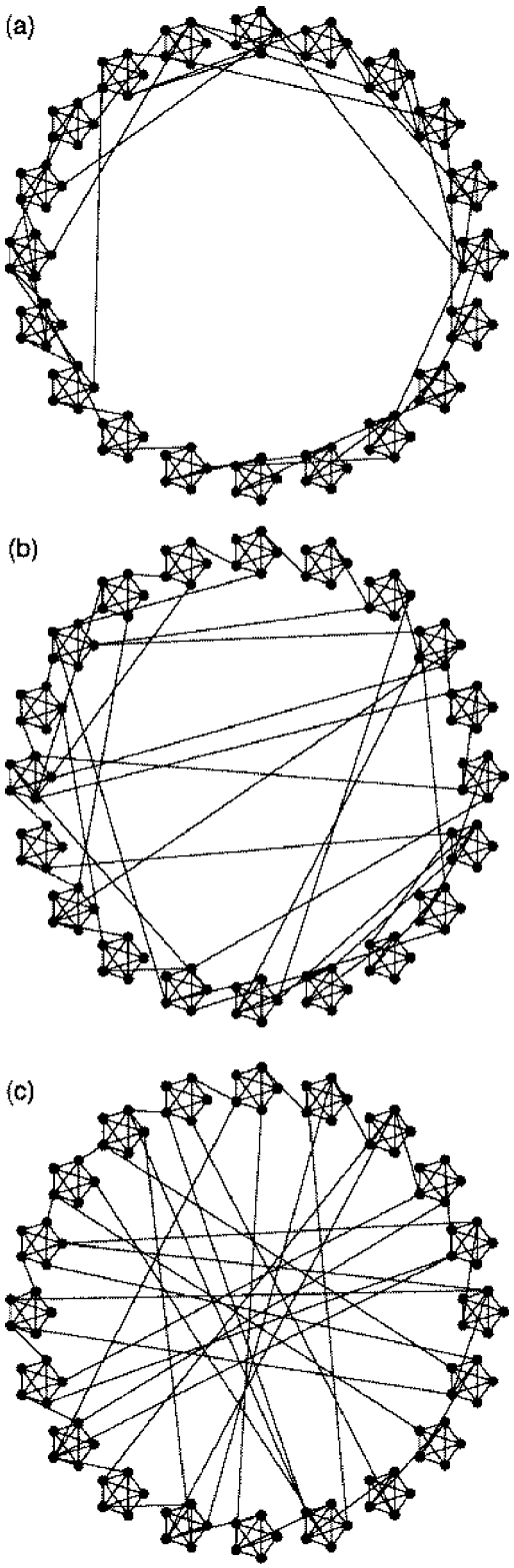

FIG. 5. Modular network configurations with different values of α: (a) $\alpha=1.0$; (b) $\alpha=0.0$; (c) $\alpha=-1.0$. Every network consists of modules with five nodes in which one-to-all connections are assumed. Neighboring modules are connected to each other to give the ring topology. The link ratio, ratio of the number of links between the modules to the total number of links in the network, is kept constant: $p=0.1$ (for the purpose of clear visualization).

decreased from a positive value to zero, and increases as α becomes negative from zero. Figure 6(b) shows the behavior of the average network distance, which is consistent with that of the eigenratio, as expected.

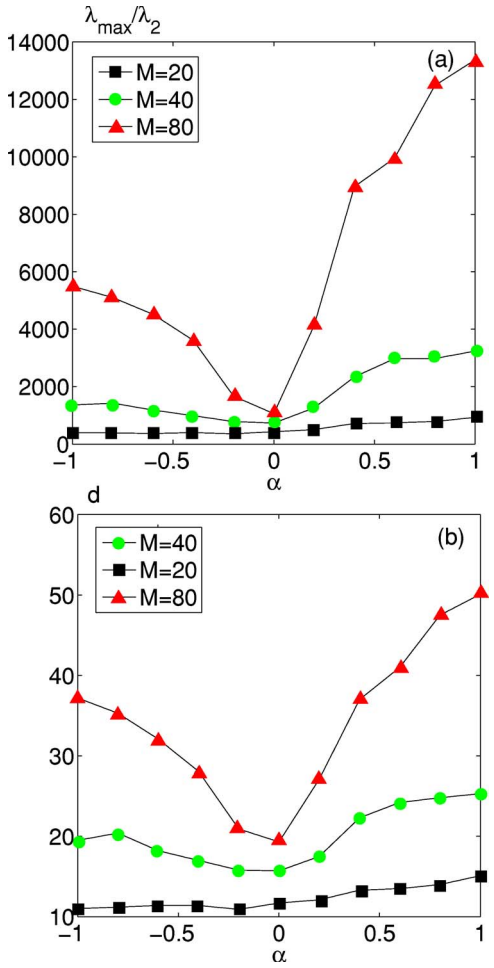

FIG. 6. (Color online) Effect of varying α on the synchronizability of ring modular network, (a) eigenratio vs α for $M=20$, 40, and 80, and (b) the corresponding average network distances vs α. All data points are averaged over 100 realizations of the network. There are five nodes per module and the link ratio is fixed at $p=0.01$.

IV. NUMERICAL SUPPORT FOR THE SYNCHRONIZABILITY TRANSITION PHENOMENON

Although our analysis of the transition phenomenon in the synchronizability of modular networks is for an idealized model, the transition is commonly observed in a variety of modular networks. In the following we present numerical support from three different modular-network models.

A. Internally scale-free modular networks

We first consider a variant of the "ring" modular networks where each individual module is a scale-free subnetwork. Connections between two modules are created in the same way as in the idealized model. That is, we choose two arbitrary modules with the probability as given by Eq. (10). Then, we randomly select a node in each chosen module and make a connection between them. The number of connections between modules is fixed so that $K_0 \approx M^{-1}$. The main difference between this class of networks and the idealized ones is that $\lambda_{\max}$ decreases with M, as shown in the inset of Fig. 7(a).

The heuristic reason for the decreasing behavior of $\lambda_{\max}$ is that the largest eigenvalue of the Laplacian matrix of

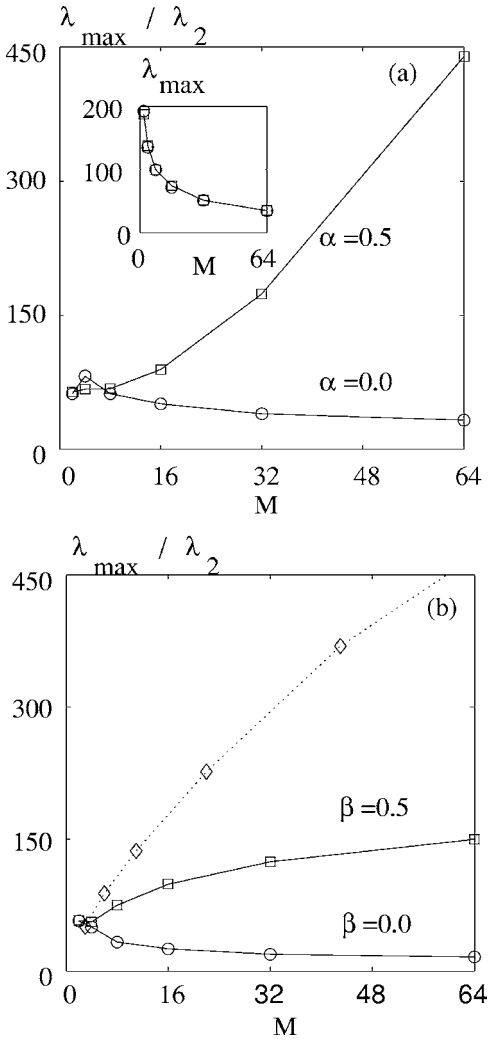

FIG. 7. Transition behavior in the synchronizability of modular networks with different modular connection structures: (a) "ring" modular networks and (b) hierarchical modular networks. Note that scalings in (a) are different from the scalings in Fig. 4, because λ_{max} is also a function of M (inset), which is a consequence of the scale-free structure within each individual module. All data points are averaged over 100 realizations of networks with $N=2048$ nodes. For comparison, the dashed line in (b) shows the corresponding behavior for a different hierarchical model, the Zachary model as described in Sec. IV C.

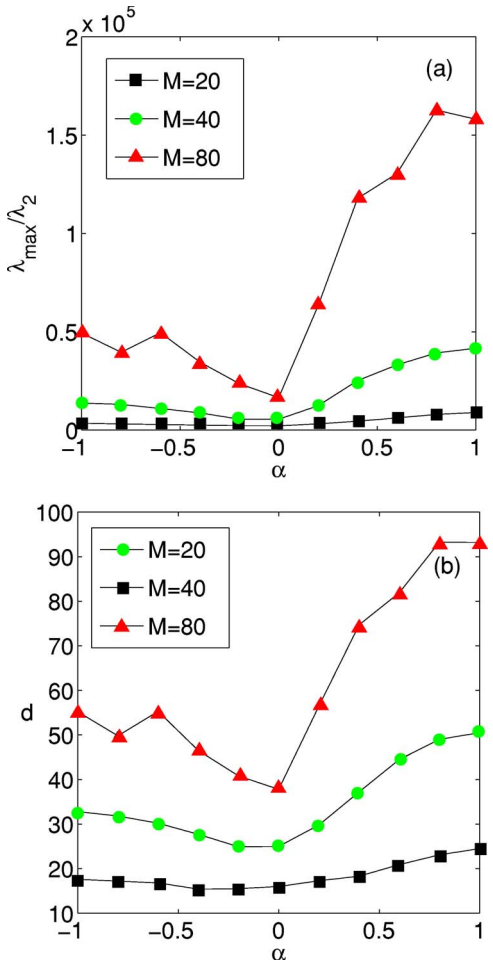

FIG. 8. (Color online) Effect of α on an internally scale-free modular networks with 50 nodes per module and link ratio $p=0.1$, (a) the eigenratio and (b) the average network distance vs α. Behaviors similar to those in Figs. 6(a) and 6(b), respectively, are observed. All data points are averaged over 100 network realizations.

scale-free networks is an increasing function of the maximum connectivity, which is proportional to the square root of the number of nodes. As the number of modules increases, the number of nodes in an individual module decreases, resulting in a decrease of the largest eigenvalue of the individual module. If there are only a few connections among modules, the largest eigenvalue of the module is almost the same as λ_{max}. Therefore, λ_{max} decreases as M increases. As in Fig. 7(a), where circles and squares represent the eigenratios of the model with $\alpha=0.0$ and $\alpha=0.5$, respectively, the networks show different behavior in synchronizability with respect to the number of modules: the synchronizability can be either enhanced or reduced by controlling the connection probability. The eigenratio and the average network distance versus α are shown in Figs. 8(a) and 8(b), respectively. We observe a qualitatively similar behavior to that in Figs. 6(a) and 6(b), respectively, which supports our heuristic argument concerning the effect of varying α on the network synchronizability.

It may be insightful to compare the synchronizability for different types of networks. To do so we have computed the eigenratios and the average network distances for a standard scale-free network (from the BA model) and for a random network, both of 4000 nodes, and compare them with a modular network of 80 modules, each of 50 nodes (the total number of nodes in the network is thus 4000). The results are listed in Table I. We observe that the modular network has larger eigenratio and larger network distance for all α than the scale-free and the random network. Although the network

TABLE I. Eigenratio and average network distance for a random network, a scale-free network, and a modular network with 80 modules, link ratio $p=0.1$, and $\alpha=0$. Each network has 4000 nodes.

	Random	SF	SF modular
Eigenratio	$\sim 5\times 10^1$	$\sim 3\times 10^2$	$\sim 2\times 10^4$
Average network distance	5.8	4.6	37

distance of random network is larger than that of SF network, the former is more synchronizable than the latter.[18]

B. Hierarchical modular networks

Our second model is a more general class of modular networks[2,20] with a hierarchical structure, where modules belong to groups which in turn belong to groups of groups, and so on. In particular, the model is motivated by social networks. Say we consider a community of N people, which represents, for instance, the population of a city. People in this community are assumed to have H relevant social characteristics that may correspond to professional or private life attributes. Each of these characteristics defines a nested hierarchical organization of groups, where people are split into smaller and smaller subgroups downwards in this nested structure.[2,20] Such a hierarchy is characterized by the number l of levels, the branching ratio b at each level, and the average number g of people in the lowest groups. Realistic values of the parameter g are on the order of tens or hundreds and represent the *average* size of typical social groups, such as groups of classmates or co-workers. The set of groups to which a person belongs defines his or her social coordinates, so that the social coordinates of person i are the positions $(x_i^1,\ldots,x_i^H)$ that this person occupies in different hierarchies. Given a hierarchy h, a distance $d(x_i^h,x_j^h)$ along h is defined for each pair of people (i,j) as the lowest level (counting from the bottom) at which i and j are found in the same group.[2,20] There is one such distance for each of the H hierarchies.

For simplicity, we consider a network dominated by only two hierarchies. The correlation between social groups is incorporated in the position a person is at in each hierarchy. The first hierarchy is constructed by assigning people randomly to the lowest groups. The second hierarchy is generated from the first by shuffling the position of each person according to a given distribution, which we assume to be exponential. Namely, each person is reassigned to a new position at distance $y\in\{1,2,\ldots,l\}$ from the original position with probability $P_\beta(y)=B\exp(-\beta y)$, where $B^{-1}=\Sigma_{k=1}^{l}\times\exp(-\beta k)$, so that the constant β characterizes the correlation between social groups. For $\beta>-\ln b$, people who are close along one hierarchy are more likely to be close along the other hierarchy as well. In the limit $\beta\gg-\ln b$, both hierarchies become identical and the model reduces to the case where $H=1$. The model in Ref. 2 corresponds approximately to the uncorrelated case where $\beta\approx-\ln b$.

Figure 7(b) shows the transition phenomenon in the synchronizability, where eigenratios of the network with $\beta=0.0$ and $\beta=0.5$ are represented by circles and squares, respectively. The networks show different behavior in synchronizability with respect to the number of modules: the synchronizability can be either enhanced or reduced by controlling the parameter β or the connection probability.

C. Zachary networks

The Zachary networks[21] were originally proposed in 1977 as a model of social network with group structures. The scale-free characteristics can be incorporated into the model by following the preferential-attachment rule proposed by Barabási and Albert.[6] There are two methods to generate a Zachary network: the growing method and the static method. In the following we shall describe these methods and present results to characterize the synchronizability of this class of modular networks.

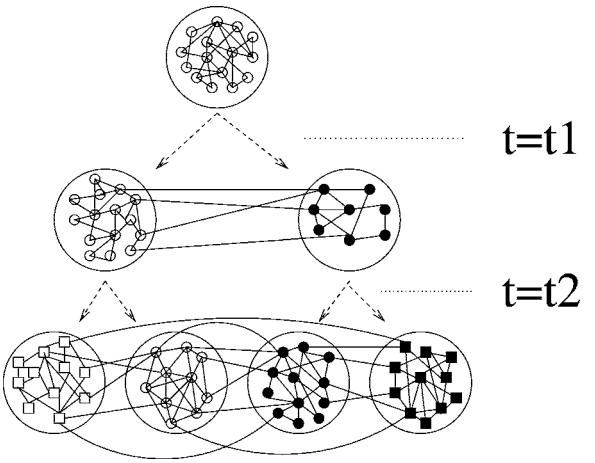

FIG. 9. The growing model for Zachary networks. Initially there exists only one module in the network. Nodes are added to the network according to the preferential-attachment rule. At time $t=t1$ the number of nodes in the initial module reaches a predefined value, and the module is divided into two submodules. Each module can grow again, divide, and so on. The growing and dividing steps continue until the total number of nodes in the network is N.

1. *Growing method*. In this method, we start from a small network with m_0 fully connected nodes. At the beginning each node is assigned the same color $\mu_i=1$, where color denotes the module to which the node belongs. At each time step a new node with m links is introduced where m is constant for all nodes, and is connected to other nodes according to the preferential attachment rule,[6] i.e., the probability that an existing node to acquire a new link is proportional to the number of links that this node already has. This new node is also assigned the color $\mu=1$. The step is repeated until the number of nodes reaches a predefined value. This step basically defines the first module, $q=1$. At the end of this step the total number of distinct colors is $q=1$. Next, we identify two nodes i and j in the group q having the largest and the second largest degree, respectively, and change the color of node j to $\mu_j=q+1$ while keeping the color of node i at $\mu_i=q$. For any remaining node $k(\neq i,j)$, its distances $d(k,i)$ and $d(k,j)$ from node i and node j (respectively) are then calculated. If node k is closer to node i, its color is assigned to be μ_i, otherwise its color is μ_j. The number of modules is equal to the number of colors. Apparently, after assigning nodes to different modules, the number of nodes in each module is reduced. To ensure that each module has the predefined number of nodes, the growth procedure is performed again for each module. Each module can be divided again to generate twice as many modules as before, and the growing mechanism can be applied again to each module, and so on. In the end, a large modular network can be generated with 2^D modules, where D is the number of divisions. This method is schematically illustrated in Fig. 9.

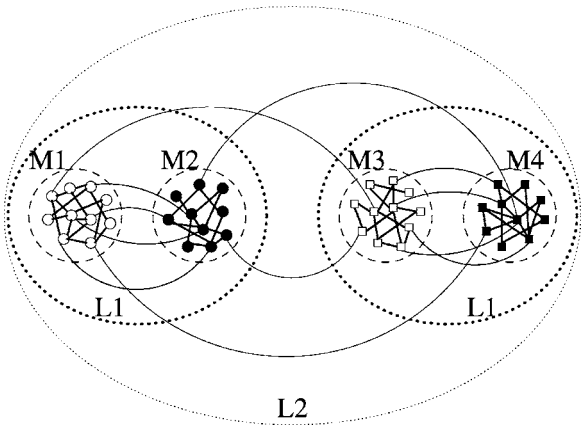

FIG. 10. A schematic illustration of the joining method. The dashed lines represent the individual modules $M1$, $M2$, $M3$, $M4$, etc., while the dotted lines represent levels $L1$, $L2$, etc., in the hierarchy (thinner lines denote a higher levels). Links are rewired according to the probability $P(l)=e^{-\beta l}$ to ensure that the resulting network possesses a hierarchical structure.

Note that in this growing method, there is no parameter that can control the probability for generating links among the modules. Thus, we cannot expect the transition phenomenon, as analyzed in Sec. III and exemplified in Fig. 4, to occur for this class of modular networks. Nonetheless, the model can be useful for testing the relation between the synchronizability and the number of modules.

2. *Joining method*. In this method, we start from a required number of modules. Let N and M be the total number of node in the entire network and the number of modules, respectively. The number of nodes in each module is thus N/M. In each module, a scale-free network of N/M nodes is formed by following the standard growth and preferential mechanisms.[6] To generate links among modules, a link in the network is chosen randomly and is detached from one of the two nodes connected by it, which has the smaller number of links. The free end of this link is to be connected to a node in a different module. This is done by choosing a module randomly and selecting a node in this module according to the preferential attachment rule. This is essentially a rewiring process. To ensure that the resulting network possesses a hierarchical structure, we group modules in pairs and form different levels of connections. Rewiring among different levels is done according to the probability $P(l)=e^{-\beta l}$, where l is an integer denoting different levels (e.g., $l=1$ means level one, and so on) and β is a parameter that controls the number of links among modules. The rewiring process is carried out until the link ratio reaches a predetermined value. This method is schematically illustrated in Fig. 10.

Note that modular networks generated by the joining method possess a hierarchical structure that can be controlled by the parameter β. It is thus possible to observe the transition phenomenon as in Fig. 4. For comparison, we set (arbitrarily) the link ratio to be $p=0.23$. Figure 11 shows the result for networks with $N=2048$ nodes and various numbers of modules. In Fig. 11(a), the network is generated by the growing method. We observe that as the number of modules is increased, the eigenratio increases proportionally, weakening the synchronizability. In Fig. 11(b), the network is generated by the joining method, and the transition phenomenon is observed. In particular, for relatively large values of β, the eigenratio exhibits a similar behavior to Fig. 11(a), i.e., it is more difficult to synchronize a network with more modules. However, for smaller values of β, the opposite trend is observed: the network synchronizability can actually be improved by increasing the number of modules. These results are consistent with our theoretical prediction based on the class of analyzable, ring modular networks (Sec. III).

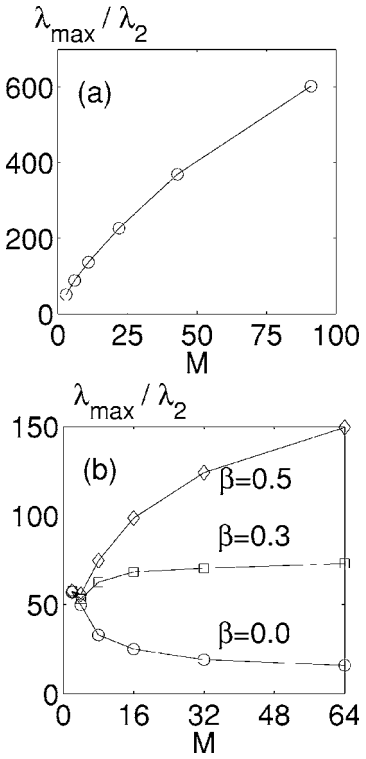

FIG. 11. Eigenratio vs the number M of modules for networks generated by (a) the growing method and (b) the joining method. In (a), the ratio increases with M. In (b), the predicted transition phenomenon is observed. The networks have $N=2048$ nodes and the data plotted are obtained using 100 random network realizations.

V. DISCUSSION

To understand the phenomenon of the synchronization in the social and biological systems with modular structure, we have investigated complex modular networks with various couplings among modules. We find that *random*, long-range couplings among modules can enhance the synchronizability, while connections among nodes within individual modules have little impact on the network's ability to synchronize. In terms of the relation between the synchronizability and the number of modules in the network, an interesting transition phenomenon is uncovered, where the network synchronizability exhibits different behaviors depending on a parameter that controls the probability of having random, long-range links among the modules. In particular, when these links are relatively less probable the synchronizability tends to deteriorate as the number of modules is increased, while the opposite occurs when the links are more probable. We have developed some theoretical understanding of this phenom-

enon based on analyzing a class of simplified networks with modules distributed according to a ring topology. These have been confirmed by extensive numerical computations. Our results imply that, in the context of social networks, a viable strategy to achieve synchronization is to devote resources to establishing and enhancing connections among distant communities.

The effect of synchronization within a modular network may be relevant to the following two situations: general election and scientific collaboration. In the first, when an election campaign starts, most citizens have little or no idea about whom they may choose among a number of candidates, but they may soon form opinions that would determine their choice of the top candidate. Global synchronization can help in this process which, dynamically, depends on the underlying modular network structure of the society. In the second example, the two seminal papers on complex networks[1,6] stimulated a wide interest in this area and led to a rapid growth of efforts. This is partly helped by some synchronization process occurring on the scientific collaboration network.

To show a potential application of our result, we speculate how an optimal way to organize collaboration networks to minimize the cost of the production may be found. In many companies, it is common that a number of workers are grouped in several divisions (modules) and collaborate to produce items. The cost of the production can be determined by the number of modules (M) and the degree of collaboration (synchronizability) among workers ($\lambda_{\max}/\lambda_2$). The cost may increase when a company needs to maintain more divisions [$f(M)$], while it may decrease when the collaboration among workers becomes better, i.e., when the eigenratio is smaller [$g(\lambda_{\max}/\lambda_2)$]. The cost of the production can therefore be defined as $C(M,\lambda_{\max}/\lambda_2)=f(M)+g(\lambda_{\max}/\lambda_2)$. Since the eigenratio $\lambda_{\max}/\lambda_2$ is in general a function of M, optimization can be accomplished when we find a value M_{opt} that minimizes the cost. As a simple example, suppose that f and g are linear functions, and the network is a globally connected "ring" as described in the caption of Fig. 4(b). Then, $C(M)=aM+b/M^2+c$, (where a, $b\geqslant 0$ and c are constants), and $M_{\mathrm{opt}}=(2b/a)^{1/3}$.

While the synchronization phenomenon studied here can be referred heuristically to as "global" (as we have focused on how all nodes in the network may become synchronized), the issue of partial synchronization within a complex network can be quite interesting. For instance, in the brain system,[22] it can be useful to have some modules or units in different modules with higher mutual synchronizability as compared to others, with low interference from other modules. Given some structural properties (connectivity), this functional bias may be achieved by different coupling strengths, and perhaps a global competitive dynamics. It may be interesting to consider the exploration of selective nonlocal synchronizability at different structural levels (units, modules) based on the method used here. These dynamics may not correspond to a globally indiscriminate synchronizability within a complex network. This form of "guided synchronizability" in complex networks may deserve further attention.

ACKNOWLEDGMENTS

This work is supported by NSF under Grant No. ITR-0312131 and by AFOSR under Grant No. F49620-01-1-0317.

APPENDIX: ALGORITHMS FOR GENERATING MODULAR NETWORKS

1. Internally scale-free modular network

1. Generate a one-dimensional ring network with M lattice points and periodic boundary conditions, where each lattice point is a module.
2. In each module, generate a SF network with n nodes by the BA model.[6]
3. Connect two nearest neighbor modules by linking one node to other, where each node is selected randomly in each module.
4. Choose two arbitrary modules with probability $P(l)=\exp(-\alpha l)/N_l$ [Eq. (10)], where l is distance between modules. Randomly select a node in each chosen module and make a connection between them.
5. Repeat step 4 until the link ratio reaches a predetermined value.

2. Hierarchical modular network with two hierarchies

1. Generate M modules in a row. Assign n nodes in the modules. All pairs of nodes in the same module are connected to each other. Distance between any pair of nodes in the same module is $y=1$.
2. Group modules in pairs as in Fig. 10, where $L1$ and $L2$ mean level $l=1$ and $l=2$, respectively. If two nodes are connected by the lowest level l, the distance between them is $y=l+1$.
3. Each node is reassigned to a new module at distance y from the original position in the first hierarchy network with probability $P_\beta=B\exp(-\beta y)$, where $B=1/\Sigma_{k=1}^{l}\exp(-\beta k)$ and β is a control parameter.

3. Zachary network

a. Growing model

1. Start with a small network with m_0 fully connected nodes. Assign color $\mu=1$ to each node.
2. Generate a SF network by the BA model, where every new node has m links and color $\mu=1$, until the number of nodes reaches a predefined value, n. This is the first module of the network, $q=1$.
3. Identify two nodes i and j in the group q having the largest and the second largest degree, respectively.
4. Change the color of node j to $\mu_j=q+1$ while keeping that of node i at $\mu_i=q$.
5. Assign color μ_i (μ_j) to node k if it is closer to node i (j).
6. Add new nodes with the same color as that of existing nodes in each module according to the growth rule of the BA model until the number of nodes reaches n in each module.

7. Divide each module again to generate twice as many modules as before.
8. Apply the growing process to each module as before.
9. Repeat the above steps until M modules are generated.

b. Joining model

1. Generate M modules in a row and then generate SF network with n nodes by the BA model in each module.
2. Group modules in pairs according to their levels (Fig. 10).
3. Choose a link randomly in the whole network and disconnect it from one of two nodes with the smaller degree.
4. Choose a different module randomly and connect the free end of the link to one of the nodes according to the preferential attachment rule.
5. Perform rewiring among different levels according to the probability $P(l)=e^{-\beta l}$, where β is a parameter.
6. Repeat the rewiring process until the link ratio reaches a predetermined value.

[1]D. J. Watts and S. H. Strogatz, Nature (London) **393**, 440 (1998).
[2]D. J. Watts, P. S. Dodds, and M. E. J. Newman, Science **296**, 1302 (2002).
[3]E. Ravasz, A. L. Somera, D. A. Mongru, Z. Oltvai, and A.-L. Barabási, Science **297**, 1551 (2002).
[4]V. Spirin and L. A. Mirny, Proc. Natl. Acad. Sci. U.S.A. **100**, 12123 (2003).
[5]G. Palla, I. Derényi, I. Farkas, and T. Vicsek, Nature (London) **435**, 814 (2005).
[6]A.-L. Barabási and R. Albert, Science **286**, 509 (1999); R. Albert and A.-L. Barabási, Rev. Mod. Phys. **74**, 47 (2002).
[7]M. Barahona and L. M. Pecora, Phys. Rev. Lett. **89**, 054101 (2002).
[8]X. F. Wang and G. Chen, Int. J. Bifurcation Chaos Appl. Sci. Eng. **12**, 187 (2002).
[9]T. Nishikawa, A. E. Motter, Y.-C. Lai, and F. C. Hoppensteadt, Phys. Rev. Lett. **91**, 014101 (2003).
[10]A. E. Motter, C. S. Zhou, and J. Kurths, Europhys. Lett. **69**, 334 (2005); Phys. Rev. E **71**, 016116 (2005).
[11]D.-U. Hwang, M. Chavez, A. Amann, and S. Boccaletti, Phys. Rev. Lett. **94**, 138701 (2005); M. Chavez, D.-U. Hwang, A. Amann, H. G. E. Hentschel, and S. Boccaletti, *ibid.* **94**, 218701 (2005).
[12]M. Girvan and M. E. J. Newman, Proc. Natl. Acad. Sci. U.S.A. **99**, 7821 (2002).
[13]E. Oh, K. Rho, H. Hong, and B. Kahng, Phys. Rev. E **72**, 047101 (2005).
[14]H. Fujisaka and T. Yamada, Prog. Theor. Phys. **69**, 32 (1983).
[15]L. M. Pecora and T. L. Carroll, Phys. Rev. Lett. **80**, 2109 (1998).
[16]K. S. Fink, G. Johnson, T. Carroll, D. Mar, and L. Pecora, Phys. Rev. E **61**, 5080 (2000).
[17]R. Monasson, Eur. Phys. J. B **12**, 555 (1999).
[18]In Ref. 9, it was shown that scale-free networks are generally more difficult to be synchronized, despite their smaller average network distances as compared with small-world networks. Intuitively, this is so mainly because of the highly heterogeneous degree distribution in scale-free networks that stipulates the existence of a small subset of nodes with extraordinarily larger numbers of links as compared with most nodes in the network. It was speculated in Ref. 9 that communication can be blocked at these nodes, reducing significantly the synchronizability of the whole network as compared with networks with more homogeneous degree distributions, such as small-world networks or random networks. However, for networks with similar characteristics, either homogeneous or heterogeneous, the average network distance (or diameter) is the determining factor for synchronizability (Ref. 8).
[19]P. Erdös and A. Rényi, Publ. Math. Inst. Hung. Acad. Sci. **5**, 17 (1960); B. Bollobaás, *Random Graphs* (Academic, London, 1985).
[20]A. E. Motter, T. Nishikawa, and Y.-C. Lai, Phys. Rev. E **68**, 036105 (2003).
[21]W. W. Zachary, J. Anthropol. Res. **33**, 452 (1977).
[22]G. Tononi, O. Sporns, and G. M. Edelman, Proc. Natl. Acad. Sci. U.S.A. **91**, 5033 (1994); **93**, 3422 (1996).